Published in final edited form as:
Nature. 2005 April 28; 434(7037): 1152–1157. doi:10.1038/nature03502.

Clathrin is required for the function of the mitotic spindle

Stephen J. Royle[1], **Nicholas A. Bright**[2], and **Leon Lagnado**[1]

[1]MRC Laboratory of Molecular Biology, Hills Road, Cambridge CB2 2QH, UK

[2]Cambridge Institute for Medical Research and Department of Clinical Biochemistry, University of Cambridge, Addenbrooke's Hospital, Hills Road, Cambridge CB2 2XY, UK

Abstract

Clathrin has an established function in the generation of vesicles that transfer membrane and proteins around the cell[1-4]. The formation of clathrin-coated vesicles occurs continuously in non-dividing cells[5], but is shut down during mitosis[6], when clathrin concentrates at the spindle apparatus[7,8]. Here we show that clathrin stabilises fibres of the mitotic spindle to aid congression of chromsomes. Clathrin bound the spindle directlyvia the N-terminal domain of clathrin heavy chain (CHC). Depletion of CHC using RNA interference prolonged mitosis; kinetochore fibres were destabilised leading to defective congression of chromosomes to the metaphase plate and persistent activation of the spindle checkpoint. Normal mitosis was rescued by clathrin triskelia but not the N-terminal domain of CHC indicating that stabilisation of kinetochore fibres was dependent on the unique structure of clathrin. The importance of clathrin for normal mitosis may be relevant to understanding human cancers that involve gene fusions of clathrin heavy chain.

Keywords

clathrin; mitosis; mitotic spindle; endocytosis; cancer; cell division

The subcellular distribution of clathrin depended on the phase of the cell cycle[7-9] (Supplementary Fig. S1). During interphase, GFP-tagged clathrin light chain a (GFP-LCa) in NRK cells was associated with the Golgi apparatus and numerous puncta representing clathrin-coated pits and vesicles[5] (Fig. 1a). But during metaphase, clathrin localised to kinetochore fibres of the mitotic spindle[10] and possibly interpolar microtubules, but not astral microtubules (Fig. 1a,b). Localisation of clathrin to kinetochore fibres was confirmed by chilling cells for 10 min at 4 °C to selectively disassemble microtubules not associated with kinetochores[11]; after this treatment, clathrin in metaphase cells remained bound to the kinetochore fibres, indicating that these microtubules were a potential site of clathrin function (Fig. 1b). Similar changes in the distribution of clathrin were observed using other variants of the light chain tagged by GFP or by immunocytochemistry using a monoclonal antibody specific for CHC (Supplementary Figs. S2,3).

Two observations indicated that clathrin bound the mitotic spindle rather than membrane localised to this region. First, none of the major adaptor proteins which allow clathrin to coat membranes (AP-1, AP-2 and AP-3)[2,3] were found at the spindle apparatus (Supplementary Fig. S4a-c). To test whether clathrin at the spindle was associated with membranes at all, we indiscriminately labelled intracellular membranes by incubating cells with the styryl dye

Correspondence and requests for materials should be addressed to S.J.R. (sjr51@mrc-lmb.cam.ac.uk).

Supplementary information accompanies the paper on www.nature.com/nature.

Competing interests statement. The authors declare that they have no competing financial interests

Europe PMC Funders Author Manuscripts

FM4-64 (15 μM) for >24 h (Supplementary Fig. S4d). In cells at metaphase, none of these membranes were found at the spindle (Fig. 1c).

The localisation of clathrin to the mitotic spindle was examined at higher resolution using immunoelectron microscopy. CHC and α-tubulin were immunolabelled with 15 nm and 10 nm colloidal gold-conjugated reagents, respectively (Fig. 1d). CHC in mitotic NRK cells was associated with the electron-dense tracks that were directed towards the chromosomes and these tracks were confirmed as microtubules by labelling for α-tubulin (Fig. 1d i and iii). CCVs were scarce in mitotic cells but when visualised (Fig. 1d ii) they could be distinguished from clathrin associated with microtubules (Fig. 1d iii). Further, clathrin immunoreactivity persisted at the spindle after soluble proteins had been removed from cells by detergent extraction (Supplementary Fig. S3). Together these results indicated that clathrin at the mitotic spindle was not coating membranes but was bound to microtubules or microtubule associated protein(s). Direct binding of CHC to the spindle apparatus has also been demonstrated by mass spectrometry[12].

To identify the region of clathrin that determined its association with the mitotic spindle, recruitment was quantified using a simple assay that compared the intensity of fluorescent proteins in the region of the spindle relative to the cytoplasm (see Methods). GFP-LCa was recruited to the spindle when CHC was abundant in cells, but not when CHC was depleted by RNAi (Fig. 2a-b), indicating that the determinant for spindle binding was contained in the heavy chain. To localise the region further, GFP-tagged fragments of CHC were expressed and their recruitment to the spindle quantified (Fig. 2c-e). CHC fragments containing the N-terminal domain (GFP-CHC(1-1074), GFP-CHC(1-479)) and the N-terminal domain itself (GFP-CHC(1-330)) were recruited, but a long construct without the N-terminal domain (GFP-CHC(331-1074) was not (Fig. 2d,e). These results indicate that clathrin triskelia bound to the mitotic spindle via the N-terminal domain of the heavy chain.

Having characterised how clathrin became associated with the mitotic spindle, we went on to investigate whether it played any role in mitosis by using RNA interference (RNAi) to deplete rat or human cells of CHC (see Supplementary Information). In NRK cells 72 h after transfection, the level of CHC in cells at interphase was ~10 % of controls and clathrin-mediated endocytosis (CME) was reduced by more than 90 % (Supplementary Fig. S5). At metaphase, the level of CHC at the spindle was 11 ± 2 % of control levels 72 h after transfection with siRNA. Depletion of CHC using RNAi also reduced proliferation of cells two-fold, even though the proportion of dead or dying cells was only ~0.3%, as judged by nuclear morphology[13,14]. Reduced proliferation was associated with prolonged mitosis, because the mitotic index was increased four-fold 72 h after CHC RNAi (rat, Fig. 3a: control 3.5 ± 0.2 %, knockdown 14.2 ± 1.1 %;human: control 1.9 ± 0.21 %, knockdown 8.4 ± 0.6; $p < 0.001$).

Did prolonged mitosis in cells depleted of CHC represent an alternative function of clathrin or an indirect effect of inhibiting CME? To investigate this question, a dominant-negative inhibitor of CME was used as an alternative method of inhibiting the established function of clathrin. When GFP-CHC(1-479) was overexpressed in NRK cells, uptake of fluorescent transferrin was inhibited by 60-70 % over the period 48-96 hours after transfection, but the mitotic index was not affected (Fig. 3b). Overexpression of GFP-CHC(1-479) inhibited CME without significantly affecting the binding of clathrin to the spindle: spindles in GFP-CHC(1-479)-expressing cells had 94 ± 6 % of the clathrin immunoreactivity observed in cells expressing GFP alone. The prolongation of mitosis in cells depleted of clathrin therefore reflected a direct action of clathrin at the mitotic spindle, distinct from its role in membrane trafficking. This conclusion was reinforced by two observations. First, CME was normally shut down during mitosis (transferrin uptake in mitotic cells was 10 ± 6 % of that

at interphase)[6]. Second, knockdown of CHC caused a series of mitotic defects (described below), none of which were observed in cells in which CME was inhibited by expression of GFP-CHC(1-479).

A number of observations indicated that clathrin regulated the congression of chromosomes. First, when we examined the proportion of cells at each stage of mitosis, more were in prometaphase after clathrin knockdown compared to controls (49 ± 6 % versus 31 ± 6 %, $p < 0.05$; Supplementary Fig. S5f). Second, the metaphase plate was thicker in cells depleted of clathrin (11.2 ± 0.9 μm compared to 7.0 ± 0.5 μm in controls, Fig. 4a) and centromeres did not organise on the mitotic spindle in an orderly manner (Fig. 4b). Third, there was an increased incidence of misaligned chromosomes in metaphase-like cells after clathrin knockdown (Fig. 4a, other examples in Fig. 4c-ii and Fig. 4e). Misaligned chromosomes were normally observed in 4 ± 1 % of rat cells at metaphase and 10 ± 7 % of human cells. But after depletion of clathrin, misaligned chromosomes were observed in only 22 ± 5 % of rat cells and 70 ± 7 % of human cells that appeared to be in metaphase. In these human cells, there was an average of 3.4 ± 0.8 misaligned chromosomes per cell. Misaligned chromosomes were usually found at spindle poles; they always consisted of pairs of sister chromatids (Fig 4d) but they did not have spindle attachments (Fig. 4c-ii) and the arms were very rarely in the "V"-shaped configuration typical of congressing chromosomes[15]. Misaligned chromosomes therefore arose due to a failure in congression during prometaphase rather than premature separation of sister chromatids.

Kinetochore fibres exert tension on sister chromatids that can be assessed by measuring the interkinetochore distance[16]. At early prometaphase, before chromosomes attach to the spindle, this distance was 0.8 ± 0.02 μm in controls and 0.8 ± 0.02 μm in cells depleted of clathrin. The upper 95 % confidence interval of the control distribution was 1.2 μm, so interkinetochore distances greater than this threshold value could be taken as evidence that the sister chromatids were under tension. Misaligned chromosomes in cells at metaphase depleted of clathrin were not under tension, because the interkinetochore distance averaged 0.9 ± 0.05 μm ($p = 0.151$). At metaphase, the interkinetochore distance of equatorial chromosomes averaged 1.6 ± 0.04 μm in control cells, but was significantly less in cells depleted of clathrin (1.3 ± 0.03 μm; $p < 0.01$). Notably, only 2 % of kinetochore pairs were at a distance less than 1.2 μm at the metaphase plate of control cells, but this increased to 20 % in cells depleted of clathrin. These results indicate that clathrin knockdown led to a reduction in tension exerted on sister chromatids of some chromosomes. Clathrin knockdown also reduced the stability of kinetochore-spindle contacts. In control cells at metaphase, all kinetochores had an attached fibre, as judged by the selective depolymerisation of microtubules not attached to kinetochores (Fig. 4c). In contrast, cells depleted of clathrin often contained "orphan" centromeres that did not have a fibre attached (Fig. 4c-i), suggesting that congression had occurred but that the fibre had been lost subsequently.

The transition from metaphase to anaphase is controlled by the spindle checkpoint, which monitors correct attachment of chromosomes to kinetochore fibres[17]. Persistent activation of the checkpoint prolongs mitosis[17]. One component of the checkpoint is Mad2, which we visualised by coupling expression of GFP-hMad2[18] to either control or CHC short hairpin RNA (shRNA) in human cells using pBrain vectors (see Methods). In cells co-expressing control shRNA, GFP-hMad2 correctly localised to kinetochores in early prometaphase (not shown) and then became diffusely distributed at metaphase[18] (Fig. 4e, left panel). But in cells co-expressing CHC shRNA, Mad2 signalling persisted during metaphase: GFP-hMad2 was found on the kinetochores of misaligned chromosomes as well as chromosomes at the metaphase plate (Fig. 4e). Staining for α-tubulin revealed that Mad2-positive kinetochores had no obvious microtubular connections (right panel of Fig. 4e). Similar observations were

made using anti-Mad2 (Supplementary Fig S7b-c). These results indicate that the primary cause of prolonged mitosis in cells depleted of clathrin was the continued activation of the spindle checkpoint that resulted from destabilisation of kinetochore microtubules.

How might clathrin influence the stability of kinetochore fibres? Free clathrin occurs as triskelia[4,19] and the N-terminal domain at the foot of each leg that is required for binding to the spindle (Fig. 2) also interacts with a large number of proteins[20,21]. One possibility is that clathrin triskelia stabilise kinetochore fibres by acting as a brace connecting 2-3 microtubules within a fibre. Alternatively, the N-terminal domain might simply recruit another protein required for stabilisation of spindle fibres. To distinguish between these two possibilities, we tested whether clathrin triskelia or the N-terminal domain alone could rescue the mitotic defects in cells depleted of endogenous clathrin. For these experiments we expressed either GFP (control), GFP-CHC(1-479) or “full-length” GFP-CHC(1-1639) in control or CHC RNAi cells, whilst making the CHC components resistant to RNAi by silent mutations in the shRNA-binding region (see Methods). For “full-length” CHC we used the major human splice variant that encodes residues 1-1639. Two observations indicated that GFP-CHC(1-1639) formed triskelia with normal function in CME. First, this construct labelled punctate structures in interphase cells and decorated the mitotic spindle at metaphase (Fig. 5a), similar to GFP-LCa[5] (Fig. 1). Second, GFP-CHC(1-1639) supported the uptake of transferrin in a manner indistinguishable from wild-type CHC (Fig. 5a,b). GFP-CHC(1-1639) also corrected mitotic defects in cells depleted of endogenous clathrin, preventing the prolongation of mitosis (Fig. 5c) and returning the incidence of misaligned chromosomes to normal levels (Fig. 5d). In contrast, the N-terminal domain alone had no significant effect on these consequences of clathrin knockdown (Fig. 5c,d). We conclude that stabilisation of kinetochore fibres required the trimeric structure of clathrin rather than the interaction function of the N-terminal domain.

Kinetochore fibres could be strengthened if clathrin triskelia form a relatively rigid connection between microtubules. In agreement with this idea, electron micrographs show microtubules within the spindle fibres to be connected by curved “bridges”[10,22], the molecular identities of which are unknown at present. These bridges result in 50-100 nm spacing between microtubules in spindle fibres[10]. By comparison, the distance between N-terminal domains of free triskelia is 45-70 nm[19,23].

We found an increased frequency of misaligned chromosomes in cells depleted of clathrin (Fig. 4,5). The mis-segregation of chromosomes during mitosis is a potential source of aneuploidy, a form of genetic instability that may lead to cancer or birth defects[24]. Given the evidence that clathrin has an alternative function in mitosis, it may be worth re-assessing the involvement of gene fusions of CHC with anaplastic lymphoma kinase (ALK)[25] in inflammatory myofibroblastic tumors and anaplastic large-cell lymphoma, as well as the fusion of CHC with transcription factor gene TFE3 in renal adenocarcinomas[26]. These gene fusions occur at the C-terminal end of CHC, and are therefore expected to disrupt trimerisation while allowing binding to the mitotic spindle. Based on our results, we suggest that these fusion proteins might impair the function of clathrin during mitosis or in the case of CHC-ALK, target a catalytically-active fragment of ALK to the mitotic spindle.

The role of clathrin in the trafficking of membrane and proteins has been studied intensively[1-3]. Here we have provided evidence for a second important function of clathrin, which occurs during mitosis – the stabilisation of kinetochore fibres of the spindle apparatus. Future studies will seek to identify protein partners for clathrin at the spindle and to understand how clathrin switches between its two functions.

Methods

See Supplementary Information for a complete description of the Methods (Molecular biology, Cell culture, Immunocytochemistry, Imaging, ImmunoEM)

Molecular biology

GFP-LCa was generated by PCR to introduce *Bgl* II and *Eco*R I sites and were subcloned into pEGFP-C1 (Clontech). GFP-CHC(1-479), GFP-CHC(1-330) and GFP-CHC(331-1074) were amplified and subcloned into *Bgl* II and *Hin*d III sites of pEGFP-C1 and GFP-CHC(1-1074) was made by subcloning a *Bgl* II-*Sca* I fragment from GFP-CHC(1-479) into GFP-CHC(331-1074). GFP-hMad2 was reconstructed to enable us to make pBrain versions (see below). GFP-hMad2 in pCS2 was amplified to introduce *Bgl* II and *Hin*d III sites and the resulting fragment was cloned into pEGFP-C1. Human CHC and clathrin light chain LCa cDNAs (I.M.A.G.E. 6187185 and 3944942) were purchased from MRC Geneservice, Cambridge, UK. GFP-tagged α-tubulin was from Clontech (pEGFP-Tub). GFP-hMad2 in pCS2[18] was a gift from Dr G. Fang (Stanford University, USA). A series of vectors (pBrain) were made that allowed the simultaneous expression of shRNA under an H1 RNA promoter and fluorescent proteins under a CMV promoter. For rescue experiments, GFP-CHC(1-479) was rendered knockdown-proof by mutation using the megaprimer method to give GFP-CHC(1-479)KDP. Knockdown-proof GFP-CHC(1-1639) was made by subcloning an *Age* I-*Mfe* I fragment into pEGFP-C1 at *Xma* I-*Mfe* I sites and then repairing the N-terminus by substituting a *Bgl* II-*Asp*718 fragment from GFP-CHC(1-479)KDP. All constructs used in this study were verified by automated DNA sequencing (Lark, UK or MRC Geneservice, UK).

Immunocytochemistry

Immunostaining was performed as described previously[27]. The following monoclonal antibodies were used: anti-clathrin heavy chain and anti-α-adaptin (X22 and AP6, Affinity BioReagents), anti-α-tubulin and anti-β1/2-adaptin (DM1A and 100/1, Sigma), anti-CENP-B was a gift from Prof. W. C. Earnshaw (University of Edinburgh, UK) and anti-δ-adaptin (clone SA4) was a gift from Prof. M. S. Robinson (Cambridge Institute for Medical Research, U.K.). Rabbit polyclonal anti-clathrin antiserum was as previously described[28]. Goat anti-mouse or anti-rabbit Cy3-conjugated secondary antibodies were from Jackson ImmunoResearch. Goat anti-mouse IgG conjugated to 10 nm colloidal gold was from Biocell. Protein A conjugated to 15 nm colloidal gold was from Department of Cell Biology, University of Utrecht. TOPRO-3 (Molecular Probes) and Hoechst 33342 (Sigma) were used for staining DNA/RNA. Uptake of Transferrin-Alexa546 (Molecular Probes) was done as previously described[29]. FM4-64 was from Calbiochem. For membrane-labelling experiments, transfected cells were cultured for >24 h in 15 μM FM4-64 at 37 °C, cells were washed for 5 min in imaging buffer (MEM without phenol red, 10% FBS, 100 U/ml pen-strep) before images were taken.

Imaging

Confocal imaging was done using a BioRad Radiance 2000 and Nikon TE300 microscope with 60x (1.4 NA) or 100x (1.3 NA) oil immersion objectives. GFP, Cy3 or FM4-64, and TOPRO-3 were excited at 488, 543, and 633 nm, respectively. For quantitative immunostaining experiments, identical laser power and acquisition settings were used. Images (8-bit) were imported into IMAGEJ (NIH) or IPLab 3.9 (Scanalytics). To quantify the uptake of transferrin-Alexa546, the outline of the cell was drawn on the GFP channel of the image and this ROI was transferred to the red channel, the image was thresholded and the number of transferrin puncta counted. Spindle recruitment was assayed by dividing the

mean pixel density measured in a 1 μm x 1 μm ROI placed over the spindle by that measured in a region outside the spindle.

The mitotic index was determined by counting the number of cells with mitotic figures as a proportion of the total number of cells within a 275 × 190 μm area. For image quantification and counting experiments, between 5-80 cells were analysed and 100-3914 cells were counted from experiments performed 3-6 times. Results are expressed as mean ± s.e.m., unpaired Student's *t*-test was used to compare control and test values and ANOVA with Dunnet's *post-hoc* test was used to compare multiple groups to a control. For binomial results (mitotic index, misaligned chromosomes, multinucleate cells etc.) data were tested for approximation to a normal distribution and *z*-values were calculated and *p*-values were retrieved using Microsoft Excel.

ImmunoEM

Cells were prepared for ultrastructural analysis using immunogold EM as previously described[30]. Briefly, mitotic NRK cells were fixed with 4 % paraformaldehyde/0.1 % glutaraldehyde in 0.1M sodium cacodylate, pH 7.2 at room temperature for 1 hour, infused with 1.7 M sucrose/15 % poly-vinyl pyrolidone and prepared as previously described[30]. Ultrathin frozen sections were collected from the knife-edge with 50:50 2 % methyl cellulose:2.3 M sucrose and immunolabelled, contrasted with methyl cellulose/uranyl acetate, dried and observed in a Philips CM100 TEM[30].

Supplementary Material

Refer to Web version on PubMed Central for supplementary material.

Acknowledgments

We thank W. C. Earnshaw, G. Fang, G. Ihrke, A. P. Jackson and M. S. Robinson for their kind gifts of antibodies, plasmids and cells. We also thank J. W. Raff and M. S. Robinson for useful discussion. This work was supported by the MRC and the Human Frontiers Science Program (Grant RGP0045/2002-C to LL). NAB was funded by the MRC.

References

1. Kirchhausen, T. Clathrin Annu. Rev. Biochem. 2000; 69:699–727. [PubMed: 10966473]
2. Brodsky FM, Chen CY, Knuehl C, Towler MC, Wakeham DE. Biological basket weaving: formation and function of clathrin-coated vesicles. Annu. Rev. Cell Dev. Biol. 2001; 17:517–68. [PubMed: 11687498]
3. Robinson MS. Adaptable adaptors for coated vesicles. Trends Cell Biol. 2004; 14:167–74. [PubMed: 15066634]
4. Fotin A, et al. Molecular model for a complete clathrin lattice from electron cryomicroscopy. Nature. 2004; 432:573–9. [PubMed: 15502812]
5. Gaidarov I, Santini F, Warren RA, Keen JH. Spatial control of coated-pit dynamics in living cells. Nat. Cell Biol. 1999; 1:1–7. [PubMed: 10559856]
6. Warren G. Membrane partitioning during cell division. Annu. Rev. Biochem. 1993; 62:323–48. [PubMed: 8352593]
7. Maro B, Johnson MH, Pickering SJ, Louvard D. Changes in the distribution of membranous organelles during mouse early development. J. Embryol. Exp. Morphol. 1985; 90:287–309. [PubMed: 3834033]
8. Okamoto CT, McKinney J, Jeng YY. Clathrin in mitotic spindles. Am. J. Physiol. Cell Physiol. 2000; 279:C369–74. [PubMed: 10913003]
9. Sutherland HG, et al. Large-scale identification of mammalian proteins localized to nuclear sub-compartments. Hum. Mol. Genet. 2001; 10:1995–2011. [PubMed: 11555636]

10. Compton DA. Spindle assembly in animal cells. Annu. Rev. Biochem. 2000; 69:95–114. [PubMed: 10966454]
11. Yao X, Abrieu A, Zheng Y, Sullivan KF, Cleveland DW. CENP-E forms a link between attachment of spindle microtubules to kinetochores and the mitotic checkpoint. Nat. Cell Biol. 2000; 2:484–91. [PubMed: 10934468]
12. Mack GJ, Compton DA. Analysis of mitotic microtubule-associated proteins using mass spectrometry identifies astrin, a spindle-associated protein. Proc. Natl. Acad. Sci. U.S.A. 2001; 98:14434–9. [PubMed: 11724960]
13. Motley A, Bright NA, Seaman MN, Robinson MS. Clathrin-mediated endocytosis in AP-2-depleted cells. J. Cell Biol. 2003; 162:909–18. [PubMed: 12952941]
14. Hinrichsen L, Harborth J, Andrees L, Weber K, Ungewickell EJ. Effect of clathrin heavy chain- and alpha-adaptin-specific small inhibitory RNAs on endocytic accessory proteins and receptor trafficking in HeLa cells. J. Biol. Chem. 2003; 278:45160–70. [PubMed: 12960147]
15. Skibbens RV, Skeen VP, Salmon ED. Directional instability of kinetochore motility during chromosome congression and segregation in mitotic newt lung cells: a push-pull mechanism. J. Cell Biol. 1993; 122:859–75. [PubMed: 8349735]
16. Waters JC, Skibbens RV, Salmon ED. Oscillating mitotic newt lung cell kinetochores are, on average, under tension and rarely push. J. Cell Sci. 1996; 109(Pt 12):2823–31. [PubMed: 9013330]
17. Cleveland DW, Mao Y, Sullivan KF. Centromeres and kinetochores: from epigenetics to mitotic checkpoint signaling. Cell. 2003; 112:407–21. [PubMed: 12600307]
18. Howell BJ, Hoffman DB, Fang G, Murray AW, Salmon ED. Visualization of Mad2 dynamics at kinetochores, along spindle fibers, and at spindle poles in living cells. J. Cell Biol. 2000; 150:1233–50. [PubMed: 10995431]
19. Ungewickell E, Branton D. Assembly units of clathrin coats. Nature. 1981; 289:420–2. [PubMed: 7464911]
20. ter Haar E, Harrison SC, Kirchhausen T. Peptide-in-groove interactions link target proteins to the beta-propeller of clathrin. Proc. Natl. Acad. Sci. U.S.A. 2000; 97:1096–100. [PubMed: 10655490]
21. Miele AE, Watson PJ, Evans PR, Traub LM, Owen DJ. Two distinct interaction motifs in amphiphysin bind two independent sites on the clathrin terminal domain beta-propeller. Nat. Struct. Mol. Biol. 2004; 11:242–8. [PubMed: 14981508]
22. Hepler PK, McIntosh JR, Cleland S. Intermicrotubule bridges in mitotic spindle apparatus. J. Cell Biol. 1970; 45:438–44. [PubMed: 5513610]
23. Kirchhausen T, Harrison SC, Heuser J. Configuration of clathrin trimers: evidence from electron microscopy. J. Ultrastruct. Mol. Struct. Res. 1986; 94:199–208. [PubMed: 3805786]
24. Jallepalli PV, Lengauer C. Chromosome segregation and cancer: cutting through the mystery. Nat Rev Cancer. 2001; 1:109–17. [PubMed: 11905802]
25. Pulford K, Morris SW, Turturro F. Anaplastic lymphoma kinase proteins in growth control and cancer. J. Cell Physiol. 2004; 199:330–58. [PubMed: 15095281]
26. Argani P, et al. A novel CLTC-TFE3 gene fusion in pediatric renal adenocarcinoma with t(X;17)(p11.2;q23). Oncogene. 2003; 22:5374–8. [PubMed: 12917640]
27. Bobanovic LK, Royle SJ, Murrell-Lagnado RD. P2X receptor trafficking in neurons is subunit specific. J. Neurosci. 2002; 22:4814–24. [PubMed: 12077178]
28. Simpson F, et al. A novel adaptor-related protein complex. J. Cell Biol. 1996; 133:749–60. [PubMed: 8666661]
29. Royle SJ, Bobanovic LK, Murrell-Lagnado RD. Identification of a non-canonical tyrosine-based endocytic motif in an ionotropic receptor. J. Biol. Chem. 2002; 277:35378–85. [PubMed: 12105201]
30. Bright NA, Reaves BJ, Mullock BM, Luzio JP. Dense core lysosomes can fuse with late endosomes and are re-formed from the resultant hybrid organelles. J. Cell Sci. 1997; 110(Pt 17): 2027–40. [PubMed: 9378754]

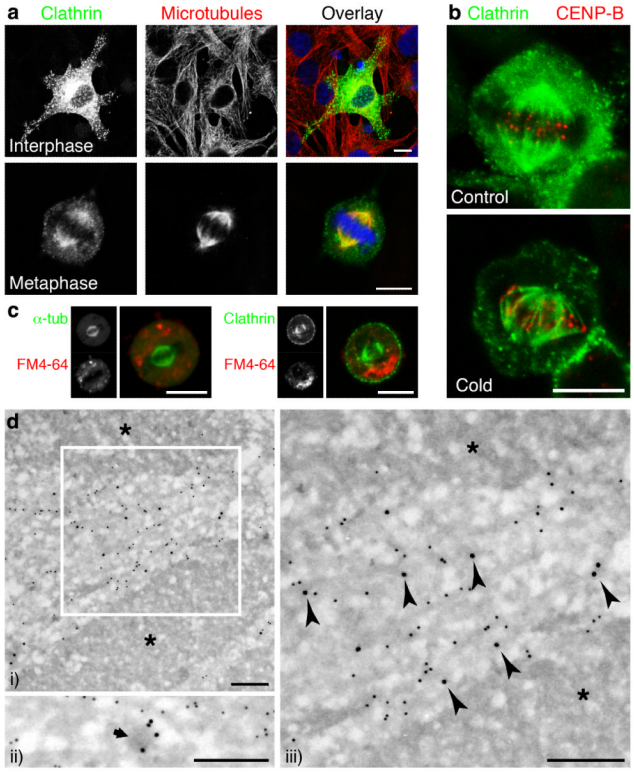

Figure 1.

Clathrin was targeted to the mitotic spindle of NRK cells. **a**, Confocal micrographs showing the subcellular distribution of clathrin at interphase and metaphase. GFP-LCa (left, green), α-tubulin (centre, red) and nucleic acids (blue). **b**, Cells expressing GFP-LCa fixed before (left) or after (right) depolymerisation of non-kinetochore microtubules. **c**-**d**, The association of clathrin with microtubules was not via coated membranes. **c**, Example images of live cells expressing either GFP-α-tubulin (left) or GFP-LCa (right) imaged following 24-28 h incubation with FM4-64 (red). **d**, Association of clathrin with microtubules visualised by immunogold EM. CHC (15 nm) and α-tubulin (10 nm gold) in mitotic NRK cells. Chromosomes are denoted by asterisks. A morphologically distinct CCV (ii) is indicated by an arrow. Arrowheads denote CHC labelling associated with microtubules. Scale bars, 10 μm (**a**-**c**) 250 nm (**d**).

Europe PMC Funders Author Manuscripts

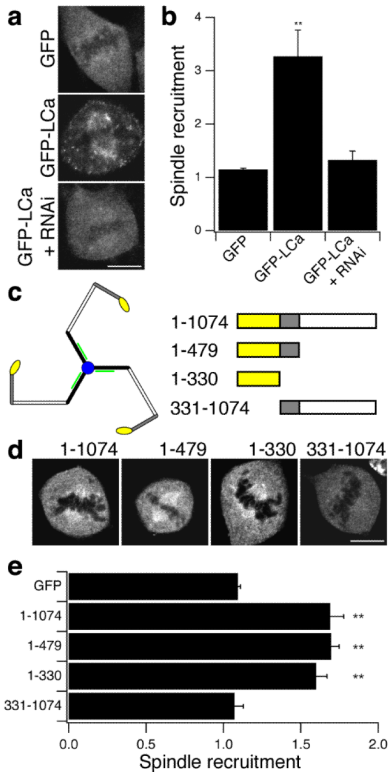

Figure 2.

Clathrin was targeted to the mitotic spindle via the N-terminal domain of the heavy chain. **a**, Example images of GFP and GFP-LCa in cells at metaphase. **b**, Histogram of spindle recruitment of GFP or GFP-LCa. A value of one represents no specific recruitment (see Methods). **c**, Schematic diagram of a clathrin triskelion and the CHC fragments used in **d**-**e** (right). CHC N-terminal domain (residues 1-330) is yellow. **d**, Example images of GFP-tagged CHC fragments in cells at metaphase. **e**, Histogram of spindle recruitment of GFP or GFP-tagged CHC fragments. Results are mean ± s.e.m, **, $p < 0.01$. Scale bars, 10 μm.

Europe PMC Funders Author Manuscripts

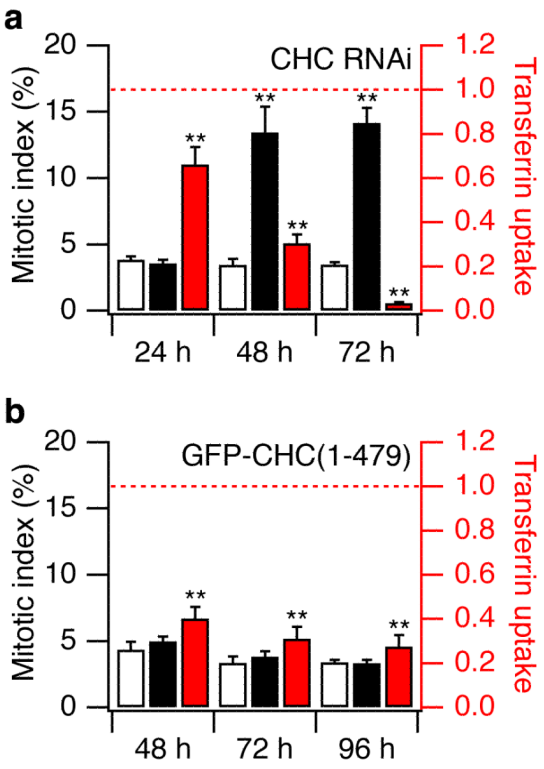

Figure 3.

Inhibition of CME did not disrupt mitosis. **a**, Effect of clathrin-depletion on mitotic index (black bars) and transferrin uptake (red bars) 24, 48 and 72 hours after transfection with CHC siRNA. Open bars show mitotic index in control siRNA-transfected cells. Transferrin uptake normalised to control values (dotted line). Within 48 hours CME was reduced by 70% and the mitotic index increased four-fold. **b**, Effects of inhibiting CME by over-expression of GFP-CHC(1-479), measured 48, 72 and 96 hours after transfection. Transferrin uptake was inhibited by 60-70%, without any change in the mitotic index. Control (open bars) was GFP alone. Results are mean ± s.e.m., **, $p < 0.01$.

Europe PMC Funders Author Manuscripts

Europe PMC Funders Author Manuscripts

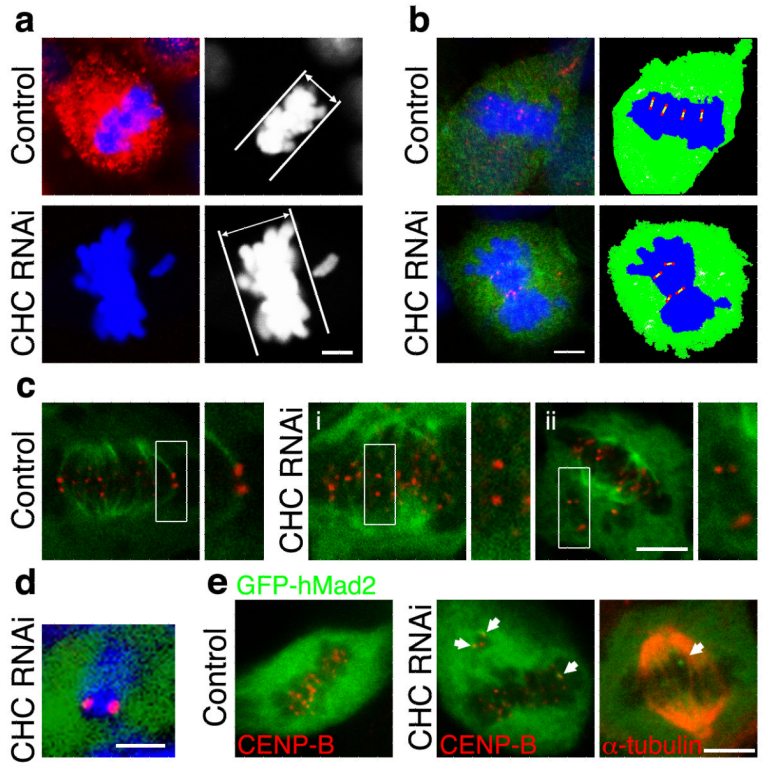

Figure 4.

Depletion of clathrin resulted in destabilised kinetochore fibres, defective congression of chromosomes and prolonged activation of the spindle checkpoint. **a**, Clathrin depletion increased the frequency of misaligned chromosomes and caused thicker metaphase plates. **b**, Clathrin-depleted metaphase-like plates were more disorganised. Cells were marked by GFP (green) stained for nucleic acids (blue) and CENP-B (red) to visualise centromeres. Schematic drawings illustrate centromere arrangement (right). **c**, Cells expressing GFP-α-tubulin (green) after depolymerisation of non-kinetochore fibres. Close-up of boxed centromere pairs (right). **d**, Misaligned chromosomes in CHC RNAi cells were pairs of sister chromatids. **e**, Representative images of one control (left) and two CHC RNAi (middle and right) cells expressing very low levels of GFP-hMad2. Mad2-positive kinetochores are indicated by arrows. Scale bars, 5 μm.

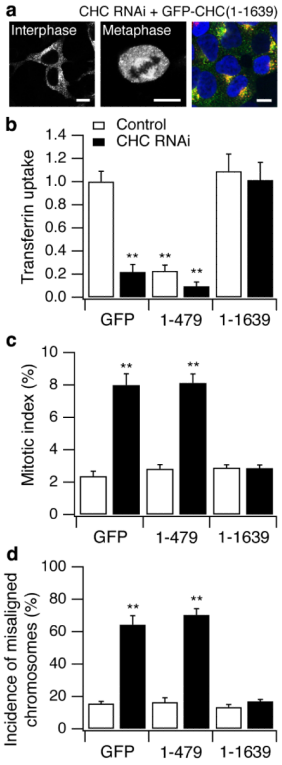

Figure 5.

"Full-length" CHC, but not CHC N-terminal domain, was sufficient to rescue the mitotic defects found in cells depleted of endogenous CHC. **a**, Representative images of GFP-tagged knockdown-proof CHC (GFP-CHC(1-1639)) expressed in HEK293 cells that were depleted of endogenous CHC. Right panel shows the normal uptake of transferrin (red) in these cells, GFP-CHC(1-1639) (green) and DNA (blue). Quantification of transferrin uptake at interphase (**b**), mitotic index (**c**) and the frequency of metaphase-like cells with misaligned chromosomes (**d**) in cells expressing GFP, GFP-CHC(1-479) or GFP-CHC(1-1639) in control cells (open bars) or cells depleted of endogenous CHC (closed bars), 72 h post-transfection.

Europe PMC Funders Author Manuscripts